New Process to Form A Nanometer to Micron Bilayer Porous Conductive 3D-Electrode Structure

Chung-Hsing Chao

Electrical And Electronic Engineering, Ta Hwa University Of Science And Technology, Hsinchu, 30743, Taiwan

Abstract: Building a nanometer to micron bilayer porosity in monolithic materials is highly desired to design 3D electrodes; however, it is still a great challenge to date. A new process to form a nanometer to micron bilayer porous conductive 3D-structure is reported herein. The process involves catalyst-free gas phase synthesis of nanotubes using acetylene gas as carbon feedstock onto a micrometer scale porous structure of carbon fiber fabric. Carbon nanotubes directly grow up on the activated sites of carbon fiber surface, which bombarded by alternate current arc discharge in a hydrogen reducing gas. And then the carbon sources originated from decomposition of diluted acetylene at temperature as low as 700~800°C using argon gases at atmospheric pressure. Helical, hollow graphitic carbons with multilevel interior structures with an outer-diameter distribution ranging from 40 nm to 130 nm, examined by scanning electron microscopy (SEM) and Raman spectroscopy, were found to be self-assembling and directly-grown on the 5-20 micrometer graphite carbon fiber surface by asymmetric alternate current sputtering and gas phase reaction. The 3D-electrode structure formed by this new process is applicable as a carbon nanomaterial cover all segments of the energy and materials sectors.

Keywords: CNTs, Carbon Fiber, CVD, Plasma.

I. INTRODUCTION

Sumio Iijima discovered multiwall nanotubes by DC arc discharge evaporation of pure graphite electrodes in Helium gas, during observation of fullerene soot [1]. Graphite, with its anisotropic two-dimensional lattice, is the stable form of carbon under ambient conditions. In the electric arc, it forms zero- and one-dimensional structures on nanometer scale, namely fullerenes and nanotubes, respectively. The nanotubes have round shaped closed tips with half-fullerene-like molecular structure. Due to their diversified molecular structures, grant an application role all 3D structures necessary to run knowledges based nanotechnology. These findings open up vast opportunities for the synthesis and study of new kinds of nanostructures with properties that may differ significantly from the corresponding bulk materials. Various potential applications have been proposed due to effective adsorbents for chromatography including separation of organic isomers, adsorbent for concentrating of substances in analysis of environmental pollutions, electrodes in batteries, and storage systems for fuels such as hydrogen and methane etc.

More recently, nanotubes could be synthesized in large scale both by the arc discharge technique and by the catalytic CVD method [2]. The graphite evaporation by a DC arc discharge in the presence of different gases produces multiwall nanotubes and carbon nanoparticles. The former are undesired products and they are difficult to eliminate. Catalytic CVD method using catalysts catalyze in the nucleation and growth of CNTs [3]. The catalytic carbon nanotube molecules grow upwards with the catalyst rooted on its base, implying catalytically active particles with high curvature sites form crystalline carbon structures out in the shape of a hemispherical dome. Dissolved or diffused carbon is then able to diffuse from inner or outer upward to create nanotubes in conjunction with the nanoparticles, elongating the structure into a hollow, seamless graphitic cylinder.

Somehow in catalytic or DC arc discharge also included the limitation at controlling the catalyst nanoparticle size and the purification of carbon nanotubes. Many of the ways used so far to control particle size, including depositing sub-nanometer metal films on surfaces, are not only difficult, expensive or time-consuming but can also give rough surfaces and large amounts of impurities such as iron (Fe), cobalt (Co), and nickel (Ni) or other transition metal catalysts, amorphous carbon deposition, which are no good for microelectronic devices. Recently, non-metallic nanoparticles have been found to synthesize catalytic CVD [3]. This development proves that the decomposition of both hydrocarbons and CNT formations are not bound to functions of catalytic metal nanoparticles [4]. Although synthesizing carbon nanotubes by catalytic CVD method is one of the widely-accepted processes in nanotube science. However, these samples did contain a large fraction of non-tubes nanoparticles such as iron (Fe), cobalt (Co), and nickel (Ni) of metals or nonmetals catalysts hard to eliminate.

We present a new process to form self-assembling CNT on the carbon fiber cloth (was purchased from CeTech Co). AC arc discharge applied on carbon fiber cloth, gives rise to create the active sites of carbon fiber, which catalytic decomposition of acetylene gas into active carbon atoms and hydrogen as low as at a relatively low temperature of 700~800°C (studies [4] have previously found that this decomposing hydrocarbon reaction would only occur at temperatures higher than 1300°C). The grown CNTs' morphology and crystallinity were characterized by SEM and Raman spectroscopy measurements. The EDX spectrum taken from the samples, from which there is no detectable metal catalyst (Fe, Co, Ni) or other impurities except for C and little O resulting from absorption, indicating pure carbon 3D nanostructures. The CNTs were confirmed to have crystalline sp^2 carbon-carbon bonds and a main peak at 26.4° attributed to the (002) diffraction of the hexagonal graphite plane, indicating the presence of CNTs with nanotube diameters averaging from 40nm to 130nm confirmed by SEM images. A little broadening nature of the peak is indicative of the long-range disorder structure of the CNTs. These samples did not contain any impurities traditionally associated with catalysts, as the high energy sites of carbon fiber replaced catalyst nanoparticles in the synthesis of self-assembling CNTs.

Experimental Method

The combined arc-discharge and chemical vapor deposition apparatus used in this study was a custom-built and modified arc-discharge furnace with an AC power supply and acetylene carbon source. The details and parameters of the experimental process can be found in a previous paper [5]. The reaction chamber was a cylindrical quartz tube with the diameter and length of 500 and 6000 mm, respectively. The anode was a dome-shaped graphite electrode with an initial diameter of 10 mm and 300 mm in length. The cathode was a graphite electrode with a U-shaped groove push fit in samples. The distance between the electrodes is reduced until the flowing of a current (50A). AC plasma is formed between the electrodes at normal pressure composed of inert and/or reactant gas. The plasma can be stabilized for a long reaction time by controlling the distance between the electrodes by means of the voltage (AC 220V, 60Hz). The reaction time varies from 20 to 30 minutes. When the AC arc discharge is carried out in the presence of hydrogen gas, the H^+ ions present in the plasma are attracted to the cathode where they form the high energy sites on the surface under ion bombardment [6]. Carbon nanotubes directly grow up on the activated sites of carbon fiber surface, which bombarded by alternate current arc discharge in a hydrogen reducing gas. And then the carbon sources originated from decomposition of diluted acetylene at temperature as low as 700~800°C using argon gases at atmospheric pressure.

A schematic illustrating in Figure 1, the steps involved in the activation of carbon fiber which bombarded by alternate current arc discharge in a hydrogen reducing gas. Nanotubes only nucleate and grow on the curvature sites under controlled pyrolysis of carbon (C^+ ion or free radicals) on the graphitic surface which bombarded by plasma, comprising the steps involved in form crystalline carbon structures out in the shape of a hemispherical dome. In dome nucleate processes of adsorption state varied from physisorption to chemisorption by chemical bonds. The driving force regarding growth processes is due to reducing surface energy. Under heterogeneous nucleation, the surface curvature sites induce less wetting angle between the surface and carbon cluster. When the dome nucleates formed, dissolved or diffused carbons being able to diffuse from the curvature sites upward elongating the structure into a hollow, seamless graphitic cylinder in conjunction with curvature filling and extension, carbon cluster stack-up, and sp^2 crystalline carbon nanotube growth with reducing Gibbs free energy.

When acetylene gas is thermally decomposed at high temperatures, it usually split into lower carbon and hydrogen or promote polymerization into higher hydrocarbons [7].

$$C_2H_{2(g)} \leftrightarrow 2C_{(s)} + H_{2(g)} \qquad\qquad (1).$$

Pyrolysis of acetylene involves simultaneous processes of complex gas-phase reactions leading to various products. This includes homogenous nucleation reaction leading to polycyclic hydrocarbons and soot and heterogeneous nucleation reaction leading to the pyrolysis gas phase carbon condensed on the fibers surface. The latter is desired reaction directly affect the nucleation and the growth of the nanotubes on the carbon fiber. In the present experiments, the former is reduced if the AC arc discharge is carried out in the presence of a hydrocarbon gas. The lowest carbon nanoparticles content in the multiwall nanotubes soot is achieved when the gas is pure hydrogen. Similar process, the graphite evaporation by a DC arc discharge in the presence of hydrocarbon, hydrogen and carrier gas produces multiwall nanotubes and nanoparticles [6]. Further, it is found that the addition of hydrogen to acetylene gas is a not only towards a reversible reaction of Equation (1) but also in formation of cyclization of acetylene in Equation (2) [7].

$$3C_2H_{2(g)} \rightarrow C_6H_{6(g)} \qquad\qquad (2).$$

The reaction is almost independent of pressure, increasing yield of benzene and hydrogen almost the same in trend with an increase of residence times. This molecular polymerization reaction of acetylene was a key factor for nanotube growth. This is due to not only decreasing carbon sources, and then pyrolysis carbon reduced as found, but also synthesizing benzene as six-membered rings of the aromatization catalysts, which belongs to a necessary step in the formation of carbon nanotubes [8]. Similar work by Zhou [9] has shown the possibility of catalyst-free growth of carbon nanotubes by a vapor-phase epitaxy method. Carbon nanotube seeds undergo air annealing and water annealing to activate their open ends. When methane or ethanol are used as a feedstock, the single-wall carbon nanotubes seeds grow. However, the growth mechanism in these conditions is not completely understood.

The grown CNTs' morphology and composition were characterized by SEM (LEO Gemini 1530) and EDX measurements, respectively. Experiment SEM images also show the surface morphologies of samples with the magnification of (A) x10000; (B) x50000; (C) x1000; (D) x1000. The image as depicted in Figure 2A, is the surface of carbon fiber before AC arc discharge. Figure 2B and 2C shows the surface where stronger etchings occured under Ar/H$_2$ ion bombardment. Figure 2D shows the growth of villi-like multiwall nanotubes around carbon fiber surface from the carbon supplied by acetylene gas. The SEM images also show a higher magnification of samples with the magnification of (A) x10000; (B) x50000; (C) x30000. Figure 3A, 3B show the images at 5 SCCM acetylene and 2.5 SCCM hydrogen. Figure 3C shows the image with a double increase of 5 SCCM hydrogen, which affected the nanostructure of multiwall nanotubes on carbon fiber (Figure 3A, 3B and 3C). The images depict a high tortuosity in the samples processed in relatively high concentrated acetylene to hydrogen along with a high density of carbon nanotubes (Figure 3A and 3B). It was found that the diameter and tortuosity of nanotubes is reduced in high concentrations of hydrogen (Figure 3C). In fact, the tortuosity of nanotubes decreases with increased hydrogen because not only the chemical reaction in Equation (1) reverses by reducing the decomposing carbon atoms but also in formation of cyclization of acetylene in Equation (2) synthesizing benzene as six-membered rings of the aromatization catalysts, which belongs to a necessary step in the formation of less kinked carbon nanotubes. Hydrogen gas in this setup affects the synthesis similar to how a small amount of water affects synthesis during catalytic CVD.

The phenomena of a kinked nanostructure can be attributed to the joining of different segments or non-hexagonal structures [10]. Kinked nanotubes are usually observed in samples made by CVD. The synthesis pentagonal-heptagonal-paired carbon rings is believed a key factor that dictates the formation mechanism of the kinked nanotubes [10] [11]. This is also introducing pentagon–heptagon defects to form a one-dimensional kinked geometry. Liu et al. [11] found that kinked multiwall nanotubes present different peculiar electronic properties from their straight ones counterparts, as electrons in the kinked structure can be localized at the irregular sites. Most interestingly, the mixture of hexagonal networks and pentagon-heptagon defects are favorable in enhancing the local chemical reactivity in comparison to the reactivity of the straight parts of multiwall carbon nanotubes, and give rise to a new potential application in the field of fuel-cell-electrode and hydrogen storage [12] [13].

In the present experiments, a nanometer to micron bilayer porous conductive 3D-structure is synthesized by AC arc discharge plasma enhanced chemical vapor deposition. The structure consists of kinked nanotubes which have branches of nanoscale diameters growing along a direction perpendicular to the carbon fiber. Prior to adding acetylene gas, ionized hydrogen ions (H$^+$) bombard carbon fiber wall and electrons discharge in arcs by the acceleration of the electric field between cathode and anode. The emitted molecule free radicals, electrons, and molecular ions under alternately electric field as depicted in figure 1. Therefore, we could see that a small amount of carbon soots deposits on the wall of quartz tube due to alternating polarity of the electrodes each cycle. Under the activation of hydrogen radicals and the plasma heating by arc discharge, the carbon atoms on the topmost surface of carbon fiber decompose, forming high energy and high curvature sites.

For nanotubes growth, the sample was heated in the center of reaction chamber. Under an AC arc discharge plasma, argon gas was firstly introduced to flush out residual gas. Subsequently, the reaction chamber was heated up to 700~800°C. Next, a mixture of acetylene gas (5 SCCM) relative to a constant (2.5 SCCM) hydrogen with an argon carrier gas (50 SCCM) was introduced. During the nanotubes growth period, the pressure value of the chamber was kept at atmospheric pressure. After 20~30 minutes, the reaction chamber was cooled down in a gas atmosphere of argon. The grain-size of the ionized bombardment on the fibers surface ranged from 10 to 100 nm under the alternating current arc-discharge and through acceleration of the electric field between cathode and anode [3]. This result can be confirmed by the as-grown hollow curved multiwall nanotubes with an outer-diameter in the range from 40 nm to 130 nm in the present study. We observed some

special structures such as curved and kinked hollow multiwall nanotubes, as seen in the inserts of the Figures 3 (A) (B) (C). These 3D nanostructures result from some degree of introduction of defects (pentagon and heptagon rings) into the normal hexagon network. In this study, these defects are likely synthesized hexagonal networks due to different reaction rate of acetylene gas (at 700~800°C) for thermal decomposing carbon atoms adsorbed on the curvature shape at the high energy sites of carbon fiber surface. This explanation is based on the premise that decomposition and absorption of carbon atoms occur on different crystalline facets of the carbon fiber surface. In addition, the growth rate of the hexagonal network determines the geometric structure of hollow carbon nanotubes by the percentage and location of pentagonal and heptagonal carbon rings.

The direct growth of multiwall nanotubes on fiber surface by AC arc discharge chemical vapor deposition was characterized by SEM and Raman spectroscopy measurements. The samples were found to contain crystalline sp^2 carbon formations with an average nanotube diameter ranging from 40 nm to 130 nm. These carbon nanotubes did not contain any impurities included catalysts because the high curvature sites of fiber replaced catalyst nanoparticles in the synthesis of nanotubes. The high curvature sites of fiber give rise to the catalytic decomposition of acetylene gas into condensed carbon atoms and hydrogen at relatively low temperature of 700~800°C. The high curvature at the surface sites of fiber provide nucleating points for the stack-up and coherence of carbon cluster, which self-assemble into nanotubes. Previous studies [14] [15] [16] have also proved that fullerene-like carbon allotropes in the form of C60, C70, C76, C82 and C84 molecules could act as nanotube seeds for synthesis single-wall carbon nanotubes by catalysis-free solid-state transformation. Liu et al. [16] has shown the nanoscale pores of carbon black: nanoscale curvatures similar to quantum dot surfaces and defect-rich structures may play an important role in the formation of carbon nanotube during catalyst-free CVD. Cai et al. [17] reported synthesis of vertically aligned carbon nanotubes without a catalyst by hydrogen arc discharge. Zuo et al. [13] used a binder-free catalyst-chemical vapor deposition method to directly growth multiwall nanotubes on carbon fiber cloth for hybrid super-capacitor applications. These samples exhibit a maximum volumetric energy density of ~4.38 mWhcm^{-3}, which is much superior to those of commercially available thin-film super-capacitors or lithium batteries. Tu et al. [18] also has found that sub-micron sized pores can directly grow hollow carbon nanorods on porous graphitic carbon film by annealing an amorphous carbon layer without catalyst. Qiu et al. [19] found a novel method to produce multiwall nanotubes from carbon spheres in a furnace at 1000 °C in a catalyst-free process. Greef et al. [20] studied the effect of the CVD parameters for direct growth of carbon nanotubes on carbon fibers. Similar results were found, as an additional pretreatment of Fe_2-Ni catalysts with a mixture gas of argon and hydrogen can improve the bamboo-like nanotubes grafted fiber yield by using the thermal decomposition of acetylene at 700°C and the equimolar acetylene-carbon dioxide reaction at 600°C.

Raman spectroscopy was used to both characterize and analyze all sp^2 carbon-based materials including graphene, carbon fibers, and carbon nanotubes. In this study, the Raman spectra were recorded on a Labram HR (Model T64000, Jobin-Yvon, Horiba group, France,) micro-spectrometer in conjunction with a confocal microscope of x50 magnification and an objective of 0.9 as the numerical aperture. The laser beam was carried out with an excitation wavelength of 632.8nm, while the beam intensity was less than 2mW. For the Raman analysis, a magnification microscope was used to select a point to focus laser beam approximately 3 μm in diameter on the sample surface. Typical exposure times for the sample ranged from 10 to 20 seconds per scan. However, static scans were also obtained in order to enhance the signal that was subsequently analysed.

A single layer of graphene or multiple layers of bulk graphite are allotropes of carbon in the stacked form of a two-dimensional, honeycomb and extraordinarily ordered lattice structure in which the two most intense features are the G band at 1580 cm^{-1} and the 2D band between 2400 and 3300cm^{-1}[21]. No D peak is observed in the center of graphene layers, which proves the absence of a significant number of defects. If a D peak is found, it would only be observed at the sample edge. Other allotropes of carbon or carbon nanotubes can be conceptualized by wrapping multiple one-atom thick layers of graphite (i.e. graphene) into a seamless cylinder of one-dimensional, hollow, and tube-like lattice structures. The typical sp2 bands are still present in the Raman spectrum of MWCNTs including the G band (1580cm^{-1}) assigned to the in-plane vibration of the carbon-carbon bond with a shoulder (approximately 1604cm^{-1}) and the D band, (1342cm^{-1}) activated by a typically defective graphite-like structure or the presence of disordered carbon-carbon bonds [22].

In Figure 4, the Raman spectrums of the multiwall nanotubes growth on fiber and the fiber base sans multiwall nanotubes accentuate the difference among the two. First, all spectrums have the two fundamental vibration modes which are observed at 1580 cm^{-1} and 1330 cm^{-1} with the G band and D band, respectively. Both of the typical vibration modes of the sp2 hybridization are present in the Raman spectrum of multiwall nanotubes-only and multiwall nanotubes-composite, including the G band (1580cm^{-1}) with a shoulder of approximately 1604cm^{-1}. However, the Raman spectrum of carbon fiber without multiwall nanotubes does not contain the peak of 1604cm^{-1}. In addition, it contains broad peaks with linewidths ranging from the 1000 cm^{-1}

mark to the 1800 cm^{-1} mark [23]. In the study, the multiwall nanotubes were separated from the surface of the carbon fiber paper using ultrasonication and the Raman spectrum was taken after drop casing the broken and dispersed multiwall nanotubes solution on a glass slide and evaporating the organic solvent.

In order to quantify and corroborate this observation, the peak poisition, peak intensity, and R (=I$_D$/I$_G$) of the first-order D and G band are given in Table 1. A little higher value around one for I$_D$/I$_G$ implies a low graphitization degree resulted from the long-range disorder structure of the multiwall nanotubes, in good agreement with the XRD results. There were no significant differences existing between the positions of the D bands. However, the G band positions were slightly changed. The position of the G band seemed to shift to a lower wavenumber due to the growth of multiwall nanotubes. This change in position is likely due to the increased edge and surface density of multiwall nanotubes compared to those of fiber alone. The I$_D$/I$_G$ ratio in Raman peak for carbon materials is related to its structure for quantifying disorder [21]. The intensity ratio of the D band to G band (I$_D$/I$_G$) of the carbon fiber without multiwall nanotubes is higher than that of the carbon fiber direct grown with multiwall nanotubes (the ratio I$_D$/I$_G$ deduced from 1.0735 to 0.9254, compared to that of carbon fiber grafted without and with bamboo-like carbon nanotubes from 0.9 to 0.83 [22]), indicating that the graphitization degree of the multiwall nanotubes composite is higher than that of carbon fiber. This observation is consistent with results found in papers by Su et al. [22] and Greef et al. [20]. The intensity ratio of the D band to G band of multiwall nanotubes seems to be higher than that of directly grown multiwall nanotubes on fibers [23]. This difference suggests the presence of a significant amount of disorder and kinked structures induced by crystalline boundaries in the sample found in multiwall nanotubes. Such a signifigant amount of disorder may have arisen from the edge of multiwall nanotubes crystallites broken off from the surface of fiber by ultrasonication. The broken edges behave in a symmetry-breaking fashion which causes D band intensity to increase.

Thermogravimetric analysis was used to examine the purity of samples and its thermal oxidation stability. Samples were characterized at a heating rate of 5ºC per minute up to 900ºC with ambient air as a carrier gas under a volume flow rate of 50 SCCM. The curve of heat flow of its weight loss also shown in this figure, revealed a single peak at 600ºC, which corresponding to the combustion temperature at its maximum weight loss. Multi-walled carbon nanotubes were oxidized beginning at 500ºC and finished off at 700ºC. There is no peak as appearing below 500ºC, which mainly corresponding to impurities of amorphous carbon, and defects. It revealed that a residue of 5.237% by weight remained after heating temperature over 700ºC, and indicated that the purity of multiwall nanotubes was 90.02% without a 4.74% of carbonaceous impurity of amorphous defects. From the TGA analysis we could directly synthesize high purity of multiwall nanotubes on fibers without the need of purification process.

II.   RESULTS AND DISCUSSION

The physical and chemical factors affecting on process are the carbon source concentration, the carbon source dispersion in inert gas, the temperature in the reactor, the promotion of the activation of AC arc discharge, and the presence of hydrogen. These factors affect the nucleation and the growth of the nanotubes, their inner, outer diameters and the orientation and the type of nanotubes. The surface morphologies of nanotubes grown at a concentration of acetylene gas of 5 SCCM in Figures 3A, 3B, and 3C differ dramatically. The image depicts high-density kinked carbon nanotubes synthesized in 5 SCCM acetylene gas and 5 SCCM hydrogen environments (Figure 3A and Figure 3B). However, in the double concentration 10 SCCM of hydrogen gas, the growth of carbon nanotubes was less tortuosity (Figure 3C). In comparison to Figure 3A and Figure 3B, the multiwall nanotubes were less tortuous and thinner in diameter due to increasing hydrogen in acetylene gas concentrations.

The multiwall nanotubes on fiber were characterized by SEM and EDS measurements. The samples were found to contain crystalline sp2 carbon formations with average nanotube diameters ranging from 40nm to 130nm. These samples did not contain iron (Fe), cobalt (Co), and nickel (Ni) or other non-metals catalysts, as the high activation sites of carbon fiber surface due to AC arc discharge plasma replaced the transition metals catalyst in this study. The new process to form multiwall nanotubes onto fiber surface was evaluated for its purity by performing elemental analysis using energy dispersive X-ray analysis (EDX). Furthermore, the crystalline structural changes for direct growth multiwall nanotubes onto fiber fabrics have been observed using Raman spectroscopy. The results proved that the crystallinity of the nanoscale multiwall nanotubes and microscale fiber of 3D bilayer composite became more ordered due to an increase in carbon-carbon bond structures.

III. CONCLUSIONS

In this study, we have developed a new process to directly grow multiwall nanotubes onto fiber exposure at a AC arc discharge plasma and chemical vapor deposition at a relatively low temperature and a catalyst free environment. The hollow, kinked shaped multiwall nanotubes have an outer-diameter ranging from 40 nm to 130 nm as follows:

1. Thermal decomposition of acetylene into carbon atoms to synthesis nanotubes on high surface energy sites of carbon fiber was carried out as low as temperature at 700~800 °C using an AC arc discharge plasma process at atmospheric pressure to be a favorable process.

2. The high energy sites of carbon fiber gives rise to provide stack-up sites for carbon atoms to deposit into self-assembling carbon nanotubes.

3. The hollow, kinked shaped multiwall nanotubes have an outer-diameter ranging from 40 nm to 130 nm.

4. Crystalline structural changes for direct growth multiwall nanotubes on the fiber have been observed to be more ordered due to the increase in carbon-carbon bond structures, which were comfirmed by Raman spectroscopy.

5. Further study is needed in order to facilitate a better plasma system to produce large area of nanotubes on carbon fiber fabrics.

ACKNOWLEDGEMENTS

REFERENCES

[1]. S. Iijima, Helical microtubules of graphitic carbon, Nature (London) 354 (1991) 56-58.
[2]. J F Colomer, C Stephan, S Fefrant, G Van Tedeloo, I Willems, Z Konya, A Fonseca, C Laurent, J Nagy, Large-scale synthesis of single-wall carbon nanotubes by catalytic chemical vapor deposition (CCVD) method, Chem. Phys. Lett. 317 (2000) 83-89.
[3]. D Takagi, H Hibino, S Suzuki, Y Kobayashi, Y Homma, Carbon nanotube growth from semiconconductor nanoparticles, Nano Lett. 7 (2007) 2272-2275.
[4]. JH Lin, C-S Chen, H-L Ma, C-W Chang, C-Y Hsu, H-W Chen, Self-assembling of multi-walled carbon nanotubes on a porous carbon surface by catalyst-free chemical vapor deposition, Carbon 46 (2008) 1611-1625.
[5]. CH Chao, W Jen, Directly grown nanotubes on carbon fiber paper in a metal-free-catalyzed chemical gas phase reaction, 2015 International Conference on Computer Science and Information Engineering (CSIE2015), June 28-29, 2015, Bangkok, Thailand.
[6]. Peter JF Harris, Solid state growth mechanisms for carbon nanotubes, Carbon 45 (2007) 229-239.
[7]. [7] K Norinaga, O Deutschmann, K-J. Huttinger, Analysis of gas phase compounds in chemical vapor deposition of carbon from light hydrocarbons, Carbon 44 (2006) 1790-1800.
[8]. RJ Song, YP Yang, Q Ji, B Li, Application of aromatization catalyst in synthesis of carbon nanotubes, Bull. Mater. Sci. 35 (2012) 33–40.
[9]. J Liu, C Wang, X Tu, B Liu, L Chen, M Zheng, C Zhou. Chirality-controlled synthesis of single-wall carbon nanotubes using vapour-phase epitaxy. Nat. Commun. 3 (2012) 1199-
[10]. R Gao, Z-L Wang, S Fan, Kinetically controlled growth of helical and zigzag shapes of carbon nanotubes, J. Phys. Chem. B 104 (2000), 1227–1234.
[11]. Liu, F Liu, J Zhao, Curved carbon nanotubes: From unique geometries to novel properties and peculiar applications, Nano Research 7 (2014) 626–657.
[12]. F Joseph, LH AuBuchon, C Chen, D Chiara, J Sungho, Multibranching Carbon Nanotubes via Self-Seeded Catalysts, Nano Lett. 6 (2006) 324–328.
[13]. W Zuo, C Wang, Y Li, J Liu, Directly Grown Nanostructured Electrodes for High Volumetric Energy Density Binder-Free Hybrid Supercapacitors: A Case Study of CNTs //Li4Ti5O12, SCIENTIC REPORTS 5 (2015) 1-8.
[14]. Y Sun, R Kitaura, J Zhang, Y Miyata, H Shinohara, Metal catalyst-free mist flow chemical vapor deposition growth of single-wall carbon nanotubes using C60 colloidal solutions, Carbon 68 (2014) 80-86.
[15]. R Qiao, RP Aaron, MS Andrew, KJ Stephen, KC Pu, Translocation of C60 and Its Derivatives Across a

Lipid Bilayer, Nano Lett. 7- 3 (2007) 614.

[16]. Y Liu, M Xu, X Zhu, M Xie, Y Su, N Hu, Z Yang, Y Zhang, Synthesis of carbon nanotubes on graphene quantum dot surface by catalyst free chemical vapor deposition, Carbon 68 (2014) 399-405.

[17]. X Cai, H Cong, C Liu, Synthesis of vertical aligned carbon nanotubes without a catalyst by hydrogen arc discharge, Carbon 50 (2012) 2726-2730.

[18]. CH Tu, CH Wu, CH Chen, YC Li, ST Wang, YC Chen, CH Lu, YJ Cai, JH Lin, Direct growth of hollow carbon nanorods on porous graphenic carbon film without catalysts, Carbon 84 (2015) 272-279.

[19]. H Qiu, G Yang, B Zhao, J Yang, Catalyst-free synthesis of multi-walled carbon nanotubes from carbon spheres and its implications for the formation mechanism, Carbon 53 (2013) 137-144.

[20]. ND Greef, L Zhang, A Magrez, L Forro, JP Locquet, I Verpoest, JW Seo, Direct growth of carbon nanotubes on carbon fibers: Effect of the CVD parameters on the degradation of mechanical properties of carbon fiber, Diamond & Related Materials 51 (2015) 39-48.

[21]. MS Dresselhaus, A Souza, M Hofmann, G Dresselhaus, R Saito, Perspectives on carbon nanotubes and graphene Raman spectroscopy, Nano Lett. 10 (2010) 751-758.

[22]. CY Su, Y Xu, W Zhang, J Zhao, A Liu, X Tang, C-H Tsai, Y Huang, LJ Li, Highly efficient restoration of graphitic structure in graphene oxide using alcohol vapors, ACS Nano 4 (2010) 5285.

[23]. AC Ferrari, JC Meyer, V Scardaci, C Casiraghi, M Lazzeri, F Mauri, S Piscanec, D Jiang, KS Novoselov, S Roth, AK Geim, Raman Spectrum of Graphene and Graphene Layers, Physical Review Letters 97 (2006) 187401-187405.

Table 1. Peak poisition, peak intensity and R(=ID/IG) values of the Laman spectrum D and G band for the test samples.

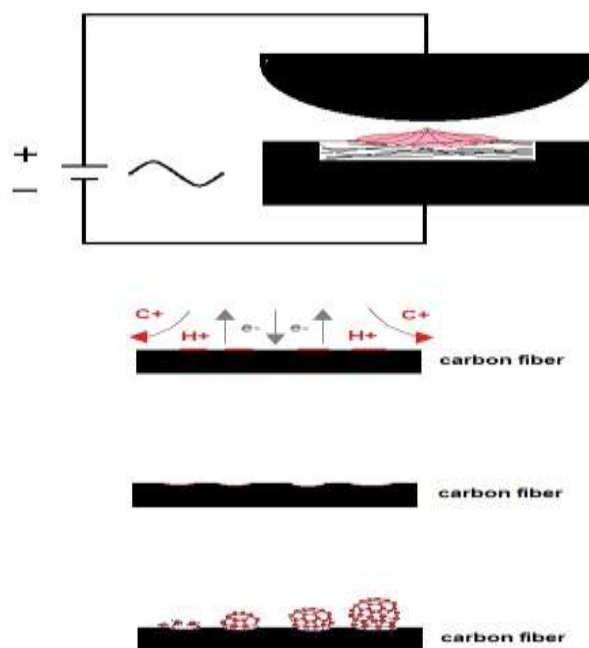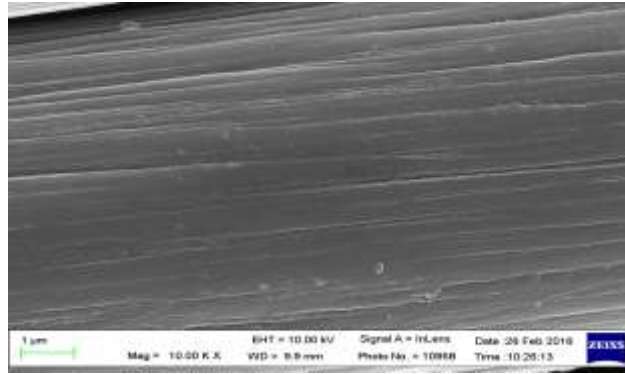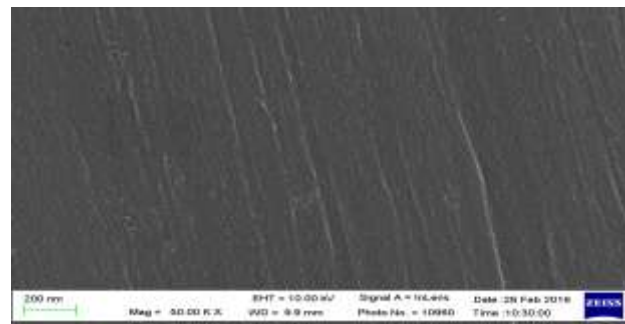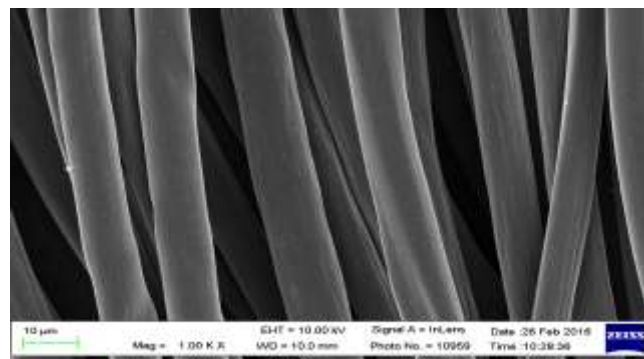| Laman Spectrum of the test samples	Peak Poisition		Peak Intensity		R
	D-band	G-band	D-band	G-band	$(=I_D/I_G)$
Fiber base	1329	1596	4699	4377	1.0735
Fiber with Multiwall Carbon Nanotubes	1330	1583	2079	2613	0.9254
Multiwall Carbon Nanotubes only	1331	1580	5491	5644	0.9728

Figure 1 Schematic illustrating the MWCNTs formation on fiber surface. (The red lines represent emitted molecules and molecular ions under alternately electric field)
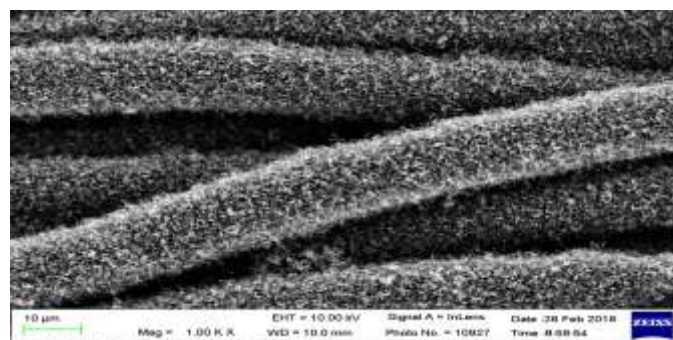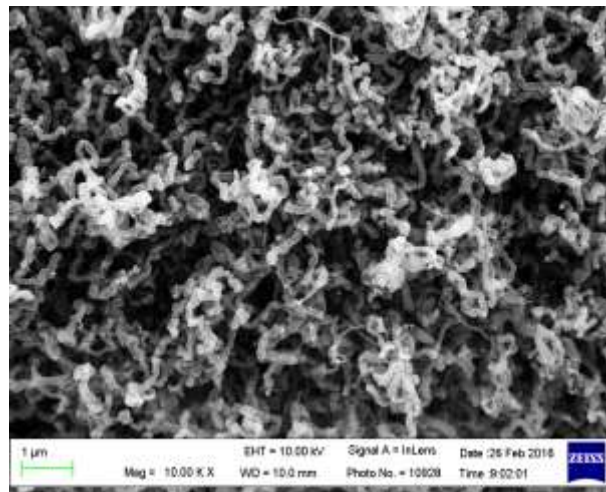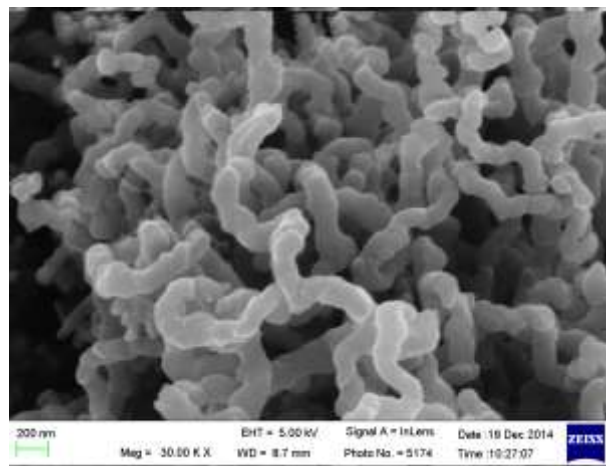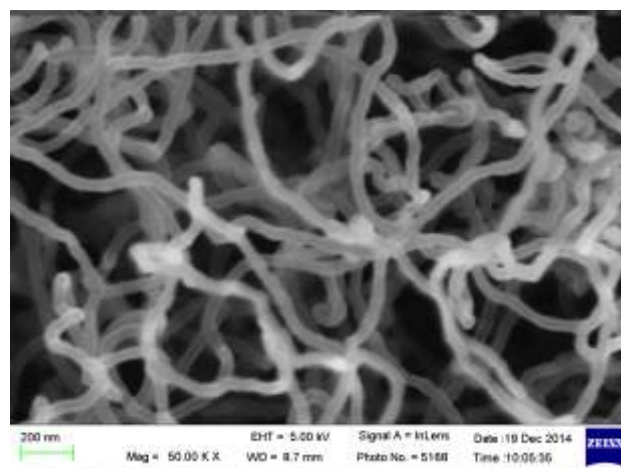
(A)

(B)

(C)

(D)

(A): scale bar = 1μm; (B): scale bar = 200 nm; (C): scale bar = 10μm; (D): scale bar = 10μm
Figure 2 A before AC arc discharge, 2B and 2C after AC arc discharge, 2D by adding acetylene gas at 700~800°C.

(A)

(B)

(C)

(A): scale bar = 1μm, (B): scale bar = 200 nm; (C): scale bar = 200 nm

Figure 3A, 3B, and 3C with a double increase in hydrocarbon gas. SEM image of fiber after AC arc discharge then CNT synthesis on the surface sites
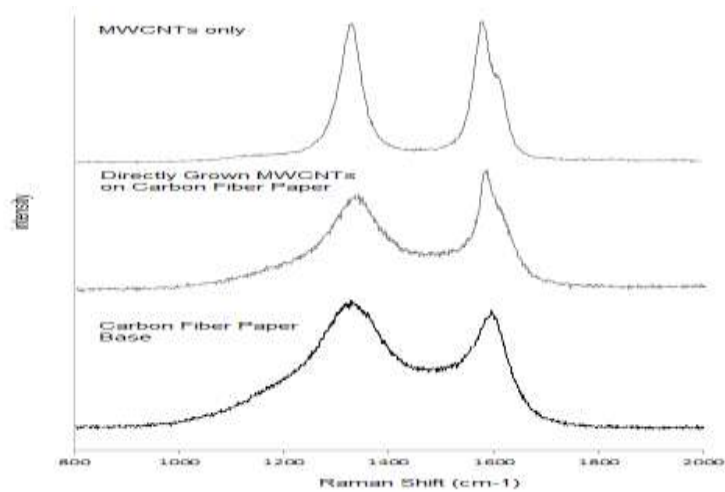
Figure 4 The D band and G band distributions for fiber base, fiber with multiwall nanotubes, and multiwall nanotubes only.
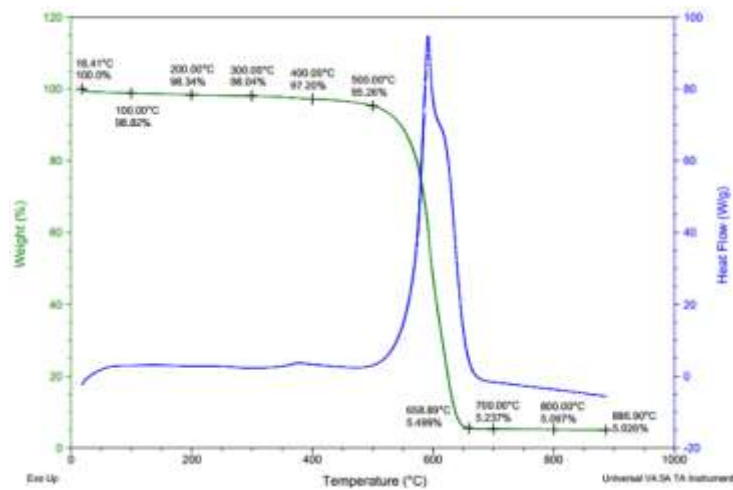

Figure 5 TAG (thermogravimetric analysis) of multiwall nanotubes samples; TGA plots of the weight percent vs. temperature (green-line) and its heat flow of the weight loss (blue-line).